Multipoint Inverse Method for Multielement Airfoil Design

Ashok Gopalarathnam* and Michael S. Selig†
University of Illinois at Urbana–Champaign, Urbana, Illinois 61801

A multipoint inverse method has been developed for the design of multielement airfoils with desired velocity distributions in incompressible potential flow. The method uses an isolated-airfoil, multipoint, inverse code to generate each element of the multielement airfoil and a two-dimensional panel method to analyze the multielement airfoil. Through Newton iteration, the variables associated with the design of the elements in isolation are adjusted to achieve desired multielement velocity distributions. As the paper demonstrates, changes in the velocity distributions over the elements in isolation result in remarkably similar changes in the velocity distributions over the corresponding elements of the multielement airfoil. This similarity results in two key features of the design method: 1) the use of the isolated airfoil velocity distributions as design variables to achieve desired distributions over the multielement airfoil, and 2) the calculation of the gradient information for the Newton iteration during the design of the isolated airfoils rather than by several panel-method analyses, resulting in substantial savings in computation time. The method thus allows rapid interactive design of multielement airfoils with desired velocity distributions, which can then be analyzed using more computationally demanding viscous codes. Examples in the paper demonstrate the capabilities of the method.

Nomenclature

C_l = airfoil lift coefficient, chord = 1
c = airfoil chord
F = vector containing the residuals
J = Jacobian matrix
n = number of design variables
V = airfoil velocity distribution normalized by freestream velocity
v = desired value of the velocity difference over a segment
ΔV = velocity difference over a segment normalized by freestream velocity
δ_f = flap deflection
δx = vector containing corrections to the design variables

Subscripts
f = property associated with the flap
IE = property associated with an element in isolation
i = index of design variable for the Newton iteration
ME = property associated with an element of a multielement airfoil
m = property associated with the main element
s = property associated with the slat

Superscript
i = step index for the Newton iteration

Introduction

T HE need for a practical inverse design method for multielement airfoils has been recognized for several decades.[1,2] Methods currently in existence are based on distribution of singularities,[3-5] conformal mapping,[6-8] or optimization formulations.[9] Several of these methods, however, are single-point methods that allow for the desired performance, e.g., velocity distribution, to be achieved at only one design point, whereas the performance at other operating points is determined by postdesign analysis. A multipoint design method, on the other hand, is capable of controlling the performance at several operating points simultaneously during the actual design effort. Airfoil design through optimization formulations can allow for multipoint design.[9] However, in spite of the significant strides made in inexpensive computation of sensitivities for the optimization[9] and simultaneous flowfield/design-parameter updating, such methods are usually computationally demanding, and the objective functions are difficult to define. Therefore, a need exists for computationally less expensive methods for rapid interactive design of multielement airfoils. Such rapid interactive methods have proven invaluable in the design of isolated airfoils and infinite cascades.[10-13] These experiences have provided the impetus to develop such a multipoint inverse method for multielement airfoils.

While the multipoint inverse methods for isolated airfoil design have been successfully based on conformal mapping and are widely used, the application of conformal mapping to the design of multielement airfoils has been less successful. Examples of methods that use conformal mapping for the design/analysis of multielement airfoils are those documented in Refs. 6–8 and 14–17. The method of James[6] for inverse design of two-element airfoils, where the flow around a two-element airfoil is mapped to the annulus between two cylinders, is a single-point design method and cannot handle more than two elements. The method of Ref. 7 is restricted to the design of a slat for a given main element. Reference 8, which builds on the analysis work of Ref. 14, shows some of the daunting challenges in developing a general multielement inverse design method based on conformal mapping. Even the more straightforward analysis problem via conformal mapping is difficult to formulate and solve.[15-17] Thus, it is believed that the mathematical challenges related to applying conformal mapping to multielement airfoil flows will continue to impede progress along these lines.

The current inverse design method uses a novel hybrid approach to avoid the difficult problem of solving the mathematical inverse problem via conformal mapping techniques, while still retaining the power and flexibility offered by the use of conformal mapping in isolated airfoil design. This is

done by coupling an isolated-airfoil inverse-design code[18,19] (PROFOIL), which is based on conformal mapping, with a two-dimensional panel method for analysis of multielement airfoils[20,21] (MCARF). The isolated airfoil design method is used to design in isolation each element of the multielement airfoil, and the panel method is used to analyze the resulting multielement airfoil. The design variables associated with the isolated airfoil design are then adjusted using Newton iteration to achieve specified inviscid velocity distributions on the multielement airfoil.

The following section describes the design method, followed by details of the Newton iteration procedure. The capabilities of the method are then demonstrated through two examples.

Design Methodology

The design methodology is illustrated using a baseline two-element airfoil as an example. It is emphasized that this and all of the remaining airfoils presented in this paper merely serve as examples and are not intended for any application. Figure 1 shows the baseline two-element airfoil at two operating conditions. (The relatively large flap element avoids small graphics, which otherwise would be hard to discern in the figures that follow.) The first operating condition corresponds to a multielement airfoil C_l of 2.0 with a flap deflection of 20 deg, and the second operating condition corresponds to a multielement airfoil C_l of 2.5, with a flap deflection of 30 deg. For this example, two cases are considered. The first case focuses on a segment on the upper surface of the main element (denoted by segment m in Fig. 1) at the first operating condition, and the second case focuses on a segment on the lower surface of the flap (denoted by segment f in Fig. 1) at the second operating condition.

Figure 2 shows an overview of the current design method. First, the individual elements of the multielement airfoil are generated using PROFOIL (step 1). In the method, each airfoil is divided into several segments. Because PROFOIL is a multipoint inverse design method, the velocity difference ΔV over any segment at some specified C_l (for the airfoil in isolation) can be prescribed during the design of the isolated airfoil. Figure 3 illustrates the definition of ΔV as used in this paper. Additional specifications may include the desired trailing-edge shapes, maximum thickness ratio for each element, and the pitching moment coefficient for each airfoil in isolation.

The resulting airfoils are then scaled and positioned according to the specified geometry for the operating points under consideration (step 2). The multielement airfoil is then analyzed at the various operating points using MCARF (step 3). The inviscid velocity difference ΔV_{ME} on the segments of the multielement airfoil, resulting from the MCARF analysis, are then compared with the corresponding specifications (step 4). It is unlikely, however, that these ΔV_{ME} values will match the specifications. To achieve the desired values of ΔV_{ME}, the isolated airfoil velocity difference ΔV_{IE} over each segment is adjusted using a Newton iteration scheme to achieve the desired multielement velocity difference ΔV_{ME} over the corresponding segments (steps 5 and 6). The isolated airfoil C_l at which the velocity difference ΔV_{IE} is evaluated is determined by the requirement that the stagnation points on the isolated airfoil and on the corresponding element of the multielement airfoil occur at the same geometric location for the multielement operating point under consideration. This requirement is necessary, particularly, when considering segments close to the leading edges of the elements.

As illustrated in Fig. 2, the method permits the designer to consider more than one arrangement of the different elements of the multielement airfoil. Thus, certain segments of the multielement airfoil can be designed for one value of C_l, while simultaneously other segments can be designed for some other value of C_l, and a third set of segments can be designed for a different location of the flap at a third C_l. This approach provides multipoint design capability to the designer.
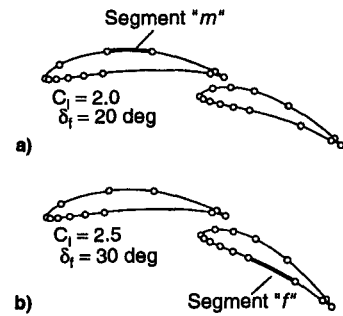

Fig. 1 Baseline two-element airfoil at the a) first and b) second operating conditions.
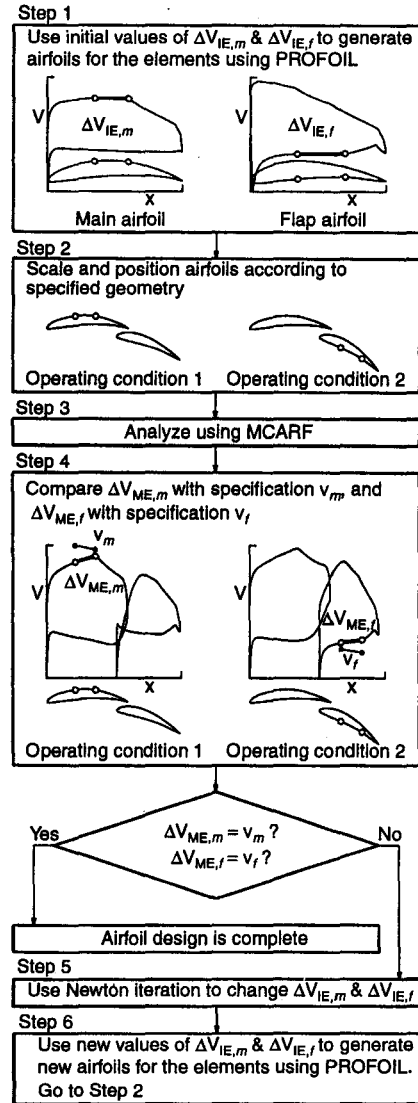

Fig. 2 Overview of the design method.

In the current design method, the multielement analysis using MCARF is done in the inviscid mode. It is recognized that viscous considerations have a significant effect on the multielement airfoil performance. However, a design method that achieves a desired inviscid velocity distribution is often the first step in a process that, when combined with more computationally intensive viscous codes, can be used to design airfoils with a desired viscous behavior.

The following example demonstrates the effectiveness of using the isolated airfoil velocity difference ΔV_{IE} over a segment to control the multielement velocity difference ΔV_{ME} over the
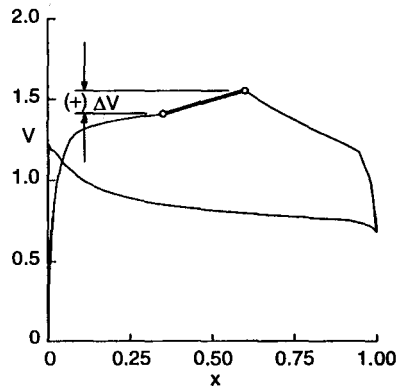
Fig. 3 Definition of ΔV for a segment as denoted by the segment endpoints.
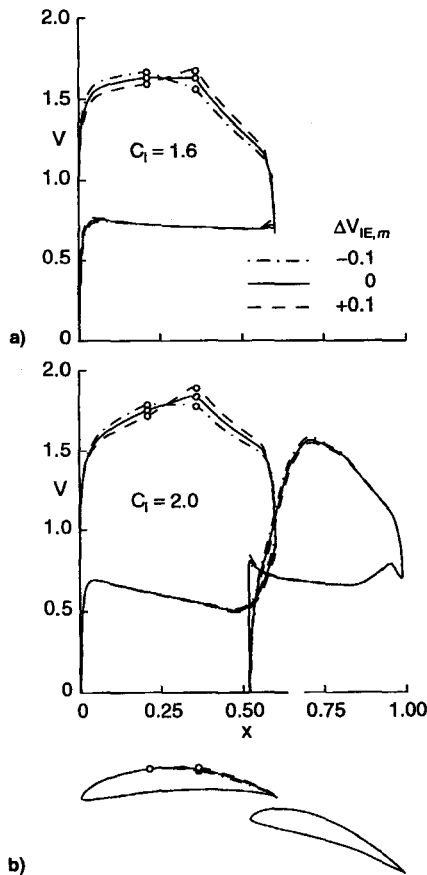

Fig. 4 Case 1: a) velocity distributions over the main element airfoils in isolation and b) multielement airfoil geometries and velocity distributions at the first operating condition.
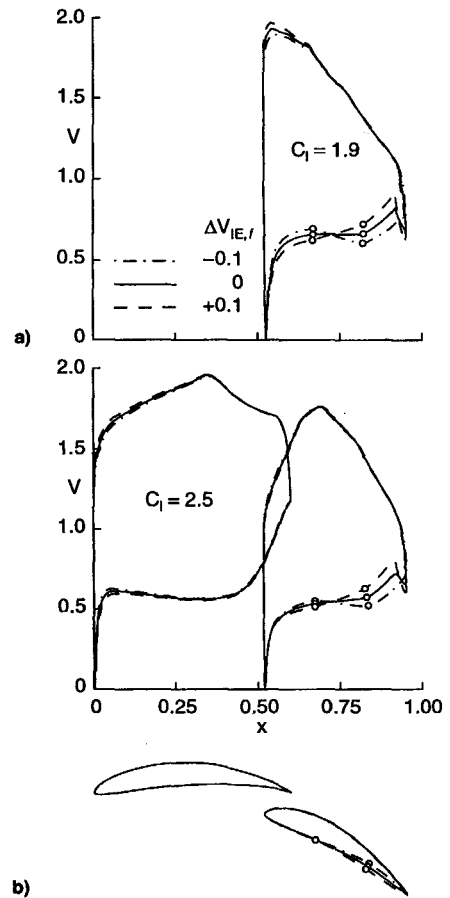

Fig. 5 Case 2: a) Velocity distributions over the flap airfoils in isolation and b) multielement airfoil geometries and velocity distributions at the second operating condition.

corresponding segment. For this demonstration, the baseline two-element airfoil of Fig. 1 is reconsidered, and the same two cases (operating conditions/segments) are examined. In each case, the ΔV_{IE} over the segment is varied to study its effect on the multielement airfoil velocity distribution, in particular, the ΔV_{ME} over the corresponding segment.

Figures 4a and 4b show the results of varying ΔV_{IE} for the segment m on the main element. Figure 4a shows three velocity distributions for the main element in isolation with $\Delta V_{IE,m} = -0.1$, 0 and $+0.1$, and $C_l = 1.6$. Figure 4b shows the three resulting multielement airfoils and the three corresponding velocity distributions for the main and flap elements of the multielement airfoil for the first operating condition. As seen in the figure the flap geometry and position are left unchanged for this case. A comparison of the velocity distributions for the

three isolated airfoils and the corresponding main elements illustrates the remarkable similarity in the trends for the three distributions. These results reveal that the isolated airfoil velocity distribution is an effective control for the velocity distribution on the corresponding element of the multielement airfoil.

Figures 5a and 5b show the results of varying $\Delta V_{IE,f}$ for the segment on the lower surface of the flap for the second operating condition, with the main element left unchanged. In this case, the velocity distributions for the main and flap elements (Fig. 5b) correspond to the second operating condition. Again, the similarity in trends between the velocity distributions on the three isolated airfoils and on the corresponding flap elements is striking.

Figures 6a and 6b show the changes in $\Delta V_{ME,m}$ and $\Delta V_{ME,f}$ resulting from perturbations to $\Delta V_{IE,m}$, with $\Delta V_{IE,f}$ kept unchanged at 0. Similarly, Figs. 6c and 6d show the changes in $\Delta V_{ME,m}$ and $\Delta V_{ME,f}$ resulting from perturbations to $\Delta V_{IE,f}$, with $\Delta V_{IE,m}$ kept unchanged at 0. Inspection of Figs. 6a–6d yields the following observations. First, perturbations to ΔV_{IE} for a particular segment result in an almost equal change in ΔV_{ME} for the same segment, that is,

$$\frac{\partial \Delta V_{ME,m}}{\partial \Delta V_{IE,m}} = \mathcal{O}(1) \tag{1a}$$

$$\frac{\partial \Delta V_{ME,f}}{\partial \Delta V_{IE,f}} = \mathcal{O}(1) \tag{1b}$$

where $\mathcal{O}(1)$ denotes of the order of 1. Second, the cross-coupling effects, such as the change in ΔV_{ME} for a segment on
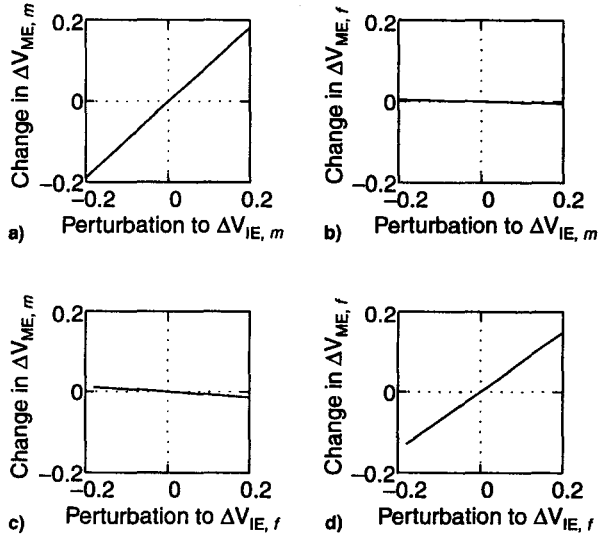
Fig. 6 Changes in $\Delta V_{ME,m}$ and $\Delta V_{ME,f}$ resulting from perturbations to $\Delta V_{IE,m}$ and $\Delta V_{IE,f}$.

one element resulting from a perturbation to ΔV_{IE} for a segment on an other element, are comparatively small, that is,

$$\frac{\partial \Delta V_{ME,m}}{\partial \Delta V_{IE,f}} \ll \frac{\partial \Delta V_{ME,m}}{\partial \Delta V_{IE,m}} \tag{2a}$$

$$\frac{\partial \Delta V_{ME,f}}{\partial \Delta V_{IE,m}} \ll \frac{\partial \Delta V_{ME,f}}{\partial \Delta V_{IE,f}} \tag{2b}$$

These results clearly show the effectiveness of using ΔV_{IE} for a segment in controlling the ΔV_{ME} for the corresponding segment. The results also show that a multidimensional Newton iteration scheme (described in greater detail in the following section) can be used to achieve desired values of ΔV_{ME} for a segment by using ΔV_{IE} for the corresponding segment as a design variable.

Newton Iteration

Typically, a system of n nonlinear equations can be solved by an n-dimensional Newton iteration, where a matrix equation is solved during each step of the iteration. In the notation used in Ref. 22, this matrix equation can be written as

$$J \cdot \delta x = -F \tag{3}$$

where F is an n-dimensional vector containing the residuals of the functions f_i to be zeroed, δx is the n-dimensional vector containing the corrections required to the n design variables x_i to bring the vector F closer to zero, and J is the $n \times n$ Jacobian of the system containing the gradient information. For each step of the iteration, F and J are determined, and δx is computed using Eq. (3). The corrections are then applied to the design variables to bring the residuals closer to zero.

Consider now, the example of Figs. 4a and 4b, where the velocity difference over a segment on the isolated main element airfoil is adjusted to achieve a desired value of the velocity difference over the corresponding segment on the main element. If this desired velocity represents the ith nonlinear equation of a larger system of n equations (for n specifications), then the residual, gradient, and correction can be expressed as

$$F_i = \Delta V_{ME,m} - v_m \tag{4}$$

$$J_{i,i} = \frac{\partial \Delta V_{ME,m}}{\partial \Delta V_{IE,m}} \tag{5}$$

$$\delta x_i = \delta(\Delta V_{IE,m}) \tag{6}$$

where v_m is the desired value of the velocity difference over the segment m on the main element.

It is seen that to compute J, one would have to evaluate the gradients numerically using a panel method. For instance, in the preceding scheme, a small perturbation is made to $\Delta V_{IE,m}$, and the resulting change in $\Delta V_{ME,m}$ is determined from a panel-method analysis. In general, for an n-dimensional Newton iteration, a panel-method analysis would have to be performed n times to determine the Jacobian for a single step in the iteration.

One major shortcoming of this approach is that calculating the Jacobian by repeated panel-method analyses is computationally very expensive, with the cost increasing with an increasing number of design variables and elements of the multielement airfoil. This cost can, however, be significantly reduced by not recomputing the influence coefficient matrix (which determines the influence of the vorticity on one panel on the flow conditions at another panel) during the gradient evaluations. Nevertheless, a method that can bypass having to perform several panel-method evaluations is likely to be computationally less expensive than the approach previously described. It is therefore worthwhile searching for an alternative scheme to compute the Jacobian without using the panel method.

With this objective in mind a re-examination of Fig. 6 reveals vital clues related to the development of an alternative scheme for computing the gradient information. As discussed earlier, the trends depicted in Fig. 6 show that a perturbation to ΔV_{IE} for a segment results in a change in ΔV_{ME} (for the corresponding segment) in the same direction. If we consider segment m, the gradient $\partial \Delta V_{ME,m}/\partial \Delta V_{IE,m}$ is always positive and approximately equal to unity.

Therefore, the high cost associated with obtaining gradient information through the panel method can be bypassed by instead obtaining the approximate gradient information using the isolated airfoil velocity difference over the segments being considered. In other words, if y_m is any design variable associated with the design of the main element airfoil, the gradient is

$$\frac{\partial \Delta V_{ME,m}}{\partial y_m} = \frac{\partial \Delta V_{ME,m}}{\partial \Delta V_{IE,m}} \frac{\partial \Delta V_{IE,m}}{\partial y_m} \tag{7}$$

If we make the approximation that $\partial \Delta V_{ME,m}/\partial \Delta V_{IE,m} \approx 1$, then Eq. (7) becomes

$$\frac{\partial \Delta V_{ME,m}}{\partial y_m} \approx \frac{\partial \Delta V_{IE,m}}{\partial y_m} \tag{8}$$

and similarly

$$\frac{\partial \Delta V_{ME,f}}{\partial y_f} \approx \frac{\partial \Delta V_{IE,f}}{\partial y_f} \tag{9}$$

These approximations to the gradients $\partial \Delta V_{IE,m}/\partial y_m$ and $\partial \Delta V_{IE,f}/\partial y_f$ can now be computed directly during the design of the isolated airfoil for the element under consideration, making it unnecessary to use the panel method for gradient calculations. Instead, the gradient information is determined through the rapid conformal mapping method used to generate the isolated airfoils. The savings in computation time resulting from the use of the approximate method of computing the gradient can be understood by comparing the CPU times for the two methods. The panel method, MCARF, typically took approximately 3.5 s for analysis of a two-element airfoil at a specified

value of C_l. On the other hand, computing a single gradient using the conformal mapping method typically took just 0.035 s (100 times faster).

By not using the panel method for computing the Jacobian, the terms coupling the main and flap elements remain uncomputed. In other words, for a design variable associated with the main element, y_m, the gradient $\partial \Delta V_{ME,f}/\partial y_m$ can be computed only by using the panel method. This gradient can be expressed as

$$\frac{\partial \Delta V_{ME,f}}{\partial y_m} = \frac{\partial \Delta V_{ME,f}}{\partial \Delta V_{IE,m}} \frac{\partial \Delta V_{IE,m}}{\partial y_m} \quad (10)$$

Using Eqs. (2a) and (2b), however, we can make the approximation that $\partial \Delta V_{ME,f}/\partial y_m \approx 0$ and $\partial \Delta V_{ME,m}/\partial y_f \approx 0$.

Thus, in the present method, the Jacobian is computed directly during the design of the isolated airfoils for the elements of the multielement airfoil. The panel-method evaluation is necessary only for computing the residuals F, reducing the number of panel-method analyses from $n + 1$ to 1 for each step of the Newton iteration.

To examine these effects in greater detail, the Jacobian can be partitioned into four submatrices, viz.,

$$J = \begin{pmatrix} J_{mm} & J_{mf} \\ J_{fm} & J_{ff} \end{pmatrix} \quad (11)$$

The submatrices J_{mm} and J_{ff} contain the gradient information on the effect of perturbing a design variable associated with an isolated airfoil on the velocity distributions over the corresponding element of the multielement airfoil. The submatrices J_{mf} and J_{fm} are the cross-coupling terms, which contain information such as those obtained by perturbing a design variable associated with the isolated airfoil of the main element on the velocity distribution over the flap element.

In the present method, J_{mm} and J_{ff} are computed directly using PROFOIL,[18,19] and J_{mf} and J_{fm} are set to zero. The justification is that the J_{mm} and J_{ff} submatrices have a much stronger contribution in driving the iterations than do J_{mf} and J_{fm}, as verified by re-examining the examples illustrated in Figs. 4 and 5 and the gradient information illustrated in Fig. 6.

For example, Fig. 4b shows that while the variation in ΔV_{IE} over a segment on the main element affects the velocity distribution on the flap, the velocity gradient on the flap is altered only slightly—in this example, over a small region near the leading edge, and on the upper surface from approximately 0.60 to $0.90c$ of the flap. If these changes tend to drive the velocity gradient away from any specified values for these regions, the ΔV_{IE} over these regions is adjusted to counter the effect and bring the velocity gradient back toward the specified values. This adjustment is done automatically by the Newton iteration.

Further reduction in computation time is achieved by observing that the Jacobian changes little as the desired solution is approached.[23] In the present implementation, the Jacobian is assumed to have converged when the maximum change in any element of the Jacobian between any two iterations is less than 1%. For further iterations, the Jacobian is not recomputed, resulting in savings in computation time.

Demonstration of the Method

The following two examples demonstrate the effectiveness of the present method in achieving specified inviscid velocity distributions on multielement airfoils. The first example demonstrates the capability of the Newton iteration scheme to converge even when there is strong coupling between the elements of a multielement airfoil. For this example, a baseline two-element airfoil (with a main and slat element) is considered at just one operating condition, corresponding to a C_l of 2.0, and the geometry shown in Fig. 7.

Two specifications are imposed on this airfoil:
1) A linear variation of 0.2 in the velocity is specified for the segment m on the upper surface of the main element, close to the leading edge.
2) A linear variation of 0.0 in the velocity is specified for the segment s on the lower surface of the slat element.

Figures 8a and 8b show the changes in $\Delta V_{ME,m}$ and $\Delta V_{ME,s}$ resulting from perturbations to $\Delta V_{IE,m}$, with $\Delta V_{IE,s}$ kept unchanged at 0. Similarly, Figs. 8c and 8d show the changes in $\Delta V_{ME,m}$ and $\Delta V_{ME,s}$ resulting from perturbations to $\Delta V_{IE,s}$, with $\Delta V_{IE,m}$ kept unchanged at 0. From Figs. 8b and 8c, it is seen that the gradient $\partial \Delta V_{ME,s}/\partial \Delta V_{IE,m} \approx -0.13$ and $\partial \Delta V_{ME,m}/\partial \Delta V_{IE,s} \approx 0.35$. This behavior is a result of the strong cross-coupling effect, arising as a result of the two segments being relatively close to each other. However, if these gradients are not evaluated using the panel method, they are both approximated to 0 during the iteration process.

Despite these approximations, the method is successful in satisfying the specifications in the velocity difference. This success is illustrated in Fig. 9, where the final velocity distri-
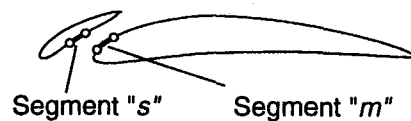

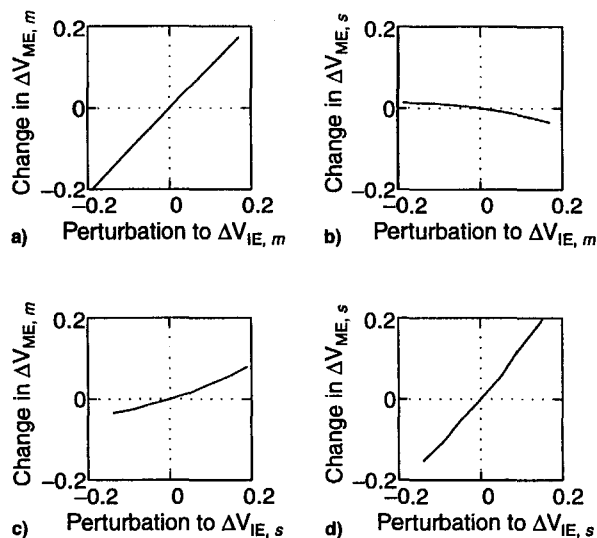**Fig. 7   Baseline two-element airfoil.**

Fig. 8   Changes in $\Delta V_{ME,m}$ and $\Delta V_{ME,s}$ resulting from perturbations to $\Delta V_{IE,m}$ and $\Delta V_{IE,s}$.
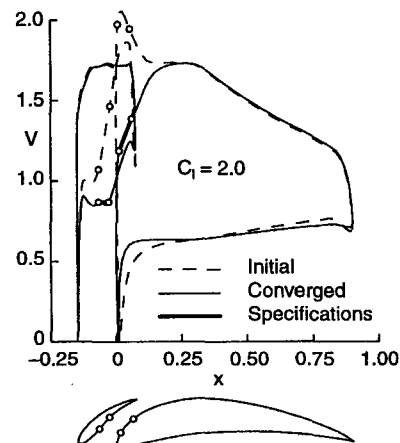

Fig. 9   Initial and converged velocity distributions on the two-element airfoil with the specifications for the two segments.

bution for the multielement airfoil at the operating condition is shown along with the specifications in the velocity difference over the two segments in consideration. Also plotted in Fig. 9 is the velocity distribution resulting from $\Delta V_{\text{IE},m} = 0.06$ and $\Delta V_{\text{IE},s} = 0.04$, which were used as initial values to start the Newton iteration.

Identical results are obtained when the panel method, MCARF is used for sensitivity computations. However, the CPU time is 905 s, which is more than six times higher than the CPU time of 134 s when PROFOIL is used for sensitivity computations. This comparison shows that, even for this simple example with just two segments under consideration, computing the approximate Jacobian using the much faster isolated airfoil design method is preferable.

The second example illustrates the multipoint capability of the method. In this example, a two-element airfoil is considered at three operating conditions. For the first two operating conditions, the flap is deflected 5 deg down relative to the main element chord line, and for the third operating condition the flap is deflected 20 deg down and is positioned further aft as compared with the 5-deg flap case. Figure 10 illustrates the locations of the elements at the three operating conditions. It must be emphasized that the airfoil shapes of the elements are not known a priori and are obtained only after the design specifications are satisfied.

The following specifications are imposed on the velocity distribution over the multi-element airfoil:

1) For the first operating condition ($\delta_f = 5$ deg), a multi-element airfoil C_l of 1.2 is considered and a linear variation in the velocity is specified over a portion of the upper surface, from 0.45 to 0.82c, of the main element (details are shown later).

2) For the second operating condition ($\delta_f = 5$ deg), a multi-element airfoil C_l of 0.5 is considered and a linear variation of velocity is specified over a portion of the lower surface, from 0.28 to 0.65c, of the main element.

3) For the third operating condition ($\delta_f = 20$ deg, with the flap moved further aft), a multielement airfoil C_l of 2.0 is considered and two specifications are made on the velocity distribution for the upper surface of the flap—constant velocity is specified over one portion (from 0.05 to 0.34c) and a linear variation is specified over another portion (from 0.54 to 0.82c) on the upper surface of the flap.

The specification made on the ΔV_{ME} for a segment is calculated from the velocities at the segment endpoints. Thus, there is no specification on the variation in velocity between the endpoints. Therefore, to accurately achieve a specification in the velocity distribution over a large region of a multielement airfoil, the region can be subdivided into several smaller segments. For this reason, the four regions for the multielement airfoil have been divided into a total of 15 segments.

Figure 11 shows the resulting airfoil shapes and the velocity distributions at the three operating conditions along with the velocity distributions for the initial airfoil shapes shown in Fig. 10, which were used to start the Newton iteration. Also shown in Fig. 11 are the velocity specifications in the four regions. As can be seen, one of the four regions is on the upper surface of the flap, close to the leading edge, where strong interactions between the elements can be expected. The method is, however, able to successfully satisfy all of the specifications. Close inspection of the numerical solution reveals that for the re-
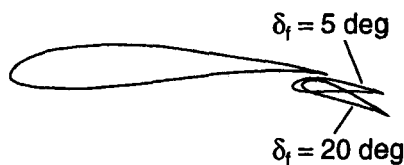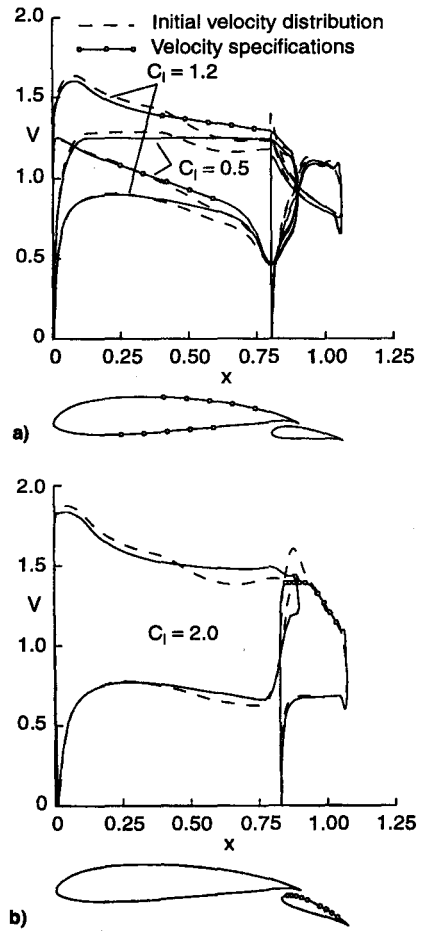
a)

b)

Fig. 11   Geometries and velocity distributions resulting from the specifications for δ_f = a) 5 and b) 20 deg.

gion on the upper surface of the flap close to the leading edge, while the specified distributions are satisfied at the segment endpoints, there are small, but nevertheless noticeable waves between the endpoints. (These waves cannot be seen in Fig. 11.) The designer can, however, achieve the specifications in the velocity distributions to any desired tolerance by dividing each portion of the airfoil into a greater number of segments. The four specified velocity distributions outlined earlier are not the only specified quantities in the design. The additional specifications include the desired trailing-edge shapes, maximum thickness ratio for each element, and the pitching moment coefficient for each airfoil in isolation. The method achieves all of these specifications using the multidimensional Newton iteration described earlier. These additional details related to the generation of the main and flap elements can be found in Refs. 18 and 19.

As a result of using the conformal mapping method instead of the panel method for computing the gradient information, the CPU time drops precipitously from 16,586 to 520 s (32 times faster), with no change in the final results. This reduction in CPU time is because of a reduction in the number of required panel-method evaluations, which drops from 4743 to just 131. This example clearly demonstrates the significance of not using the panel method for computing the gradient information.

Finally, although the multielement airfoil examples used in this paper consists of two elements, the method and the code can be readily used for the design of several elements at arbitrary locations (multiple flaps and slats). This makes the method useful in a wide variety of applications.

Conclusions

A multipoint design method for multielement airfoils has been developed. The method allows the designer to specify

Fig. 10   Locations of the elements for the example multielement airfoil.

desired inviscid velocity distributions over the multielement airfoil in a multipoint fashion by coupling an isolated airfoil multipoint design code with a panel method. The isolated airfoil code is used to generate the airfoil shape for each element of the multielement airfoil, and the panel method is subsequently used to analyze the resulting multielement airfoil. Through Newton iteration, the variables associated with the design of the isolated airfoils are adjusted to achieve desired velocity gradients over the multielement airfoil.

The paper discusses an important observation on the similarity in trends in the change in velocity gradients for an airfoil in isolation and as a part of a multielement airfoil. This observation is used to great effect to arrive at two key features of the method: 1) the use of the isolated airfoil velocity distributions as design variables to achieve desired velocity distributions over the multielement airfoil and 2) a scheme to compute gradient information for the Newton iteration during the design of the isolated airfoils rather than by several panel-method analyses. These two features make the method highly efficient, thereby allowing for rapid interactive design of multielement airfoils.

As the examples demonstrate, the method provides the capability to specify different inviscid velocity distributions over different portions of the airfoil, not only at multiple values of the lift coefficient, but also at multiple locations of the elements of the multielement airfoil. Thus, the method is particularly suited to achieving desired inviscid behavior prior to using more computationally intensive codes to analyze the viscous behavior. Also, by the addition of an integral boundary-layer method, it is conceivable that the current method can be extended to handle viscous inverse design of multielement airfoils.

Acknowledgments

References

[1]Smith, A. M. O., "High-Lift Aerodynamics," *Journal of Aircraft*, Vol. 12, No. 9, 1975, pp. 501–530.

[2]Brune, G. W., and McMasters, J. H., "Computational Aerodynamics Applied to High-Lift Systems," *Applied Computational Aerodynamics*, edited by P. A. Henne, Vol. 125, Progress in Astronautics and Aeronautics, AIAA, Washington, DC, 1990, pp. 389–433.

[3]Narramore, J. C., and Beatty, T. D., "An Inverse Method for the Design of Multi-Element High-Lift Systems," AIAA Paper 75-879, June 1975.

[4]Kennedy, J. L., and Marsden, D. J., "A Potential Flow Design Method for Multicomponent Airfoil Sections," *Journal of Aircraft*, Vol. 15, No. 1, 1978, pp. 47–52.

[5]Bristow, D. R., "Improvements in Surface Singularity Analysis and Design Methods," *Advanced Technology Airfoil Research*, Vol. 1, NASA CP-2045, Pt. 1, March 1978, pp. 221–236.

[6]James, R. M., "The Theory and Design of Two-Airfoil Lifting Systems," *Computer Methods in Applied Mechanics and Engineering*, Vol. 10, No. 1, 1977, pp. 13–43.

[7]O'Pray, J. E., and Lissaman, P. B. S., "Slat Design by a Semi-Inverse Technique," AIAA Paper 71-11, Jan. 1971.

[8]Prosnak, W. J., "The Inverse Problem for Multiconnected Airfoil Systems," *Recent Developments in Theoretical and Experimental Fluid Mechanics, Compressible and Incompressible Flows*, edited by U. Müller, K. G. Roesner, and B. Schmidt, Springer–Verlag, New York, 1979, pp. 517–528.

[9]Drela, M., "Design and Optimization Method for Multi-Element Airfoils," AIAA Paper 93-0969, Feb. 1993.

[10]Eppler, R., *Airfoil Design and Data*, Springer–Verlag, New York, 1990.

[11]Selig, M. S., Maughmer, M. D., and Somers, D. M., "A Natural-Laminar-Flow Airfoil for General-Aviation Applications," *Journal of Aircraft*, Vol. 32, No. 4, 1995, pp. 710–715.

[12]Selig, M. S., "Multipoint Inverse Design of an Infinite Cascade of Airfoils," *AIAA Journal*, Vol. 32, No. 4, 1994, pp. 774–782.

[13]Selig, M. S., and Guglielmo, J. J., "High-Lift Low Reynolds Number Airfoil Design," *Journal of Aircraft*, Vol. 34, No.1, 1997, pp. 72–79.

[14]Prosnak, W. J., and Klonowska, M. E., "Closed Formulae for Aerodynamic Coefficients of Arbitrary Biplane Wing Sections," *Zeitschrift für Angewandte Mathematik und Mechanik*, Vol. 57, No. 1, 1997, pp. 25–31.

[15]Ives, D. C., and Liutermoza, J. F., "Analysis of Transonic Cascade Flow Using Conformal Mapping and Relaxation Techniques," *AIAA Journal*, Vol. 15, No. 5, 1977, pp. 647–650.

[16]Garrick, I. E., "Potential Flow About Arbitrary Biplane Wing Sections," NACA Rept. 542, 1936.

[17]Halsey, N. D., "Potential Flow Analysis of Multielement Airfoils Using Conformal Mapping," *AIAA Journal*, Vol. 17, No. 12, 1979, pp. 1281–1288.

[18]Selig, M. S., and Maughmer, M. D., "A Multi-Point Inverse Airfoil Design Method Based on Conformal Mapping," *AIAA Journal*, Vol. 30, No. 5, 1992, pp. 1162–1170.

[19]Selig, M. S., and Maughmer, M. D., "Generalized Multipoint Inverse Airfoil Design," *AIAA Journal*, Vol. 30, No. 11, 1992, pp. 2618–2625.

[20]Stevens, W. A., Goradia, S. H., and Braden, J. A., "Mathematical Model for Two-Dimensional Multi-Component Airfoils in Viscous Flows," NASA CR-1843, July 1971.

[21]Morgan, H. L., Jr., "A Computer Program for the Analysis of Multi-Element Airfoils in Two-Dimensional, Subsonic, Viscous Flow," NASA SP-347, March 1975.

[22]Press, W. H., Teukolsky, S. A., Vetterling, W. T., and Flannery, B. P., *Numerical Recipes in Fortran—The Art of Scientific Computing*, 2nd Ed., Cambridge Univ. Press, New York, 1992, pp. 372–375.

[23]Ferziger, J. L., *Numerical Methods for Engineering Applications*, Wiley, New York, 1981, pp. 258–259.